AIAA 2002-0984

# On the Development of a Subgrid Scale Clutter Model

P.E. DesJardin, J. M. Nelsen, L. A. Gritzo
Sandia National Laboratories
Albuquerque, NM 87185

T. A. Ghee
NAVAIR
Patuxent River, MD 20670

40th AIAA Aerospace Sciences Meeting and Exhibit
January 14-17, 2002
Reno, NV

# ON THE DEVELOPMENT OF A SUBGRID SCALE MODEL FOR CLUTTER

**Paul E. DesJardin, James M. Nelsen and Louis A. Gritzo**
Fire Science and Technology
Sandia National Laboratories*
Albuquerque, NM 87185

**Terry A. Ghee**
NAVAIR
Patuxent River, MD 20670

## Abstract

The objective of this research is to develop a subgrid scale model to account for the effects of small objects, or "clutter", that are difficult to resolve using a CFD mesh. These objects may range in size from being small relative to the grid (*i.e.* porous media limit) to scales, which are on the same order as the grid size (*i.e.* a bluff body limit). Transport equations for momentum, turbulent kinetic energy and turbulent kinetic energy dissipation rate are derived based on time and spatial filtering concepts, introducing unknown correlations and surface integral terms that require explicit subgrid scale (SGS) model closures. The SGS models are formulated using a combination of well-established constitutive relations borrowed from the porous media literature and classical relations for drag on bluff bodies. The modeling methodology is exercised for two classes of problems. The first is flow in a porous media for which the obstructions are relatively dense. For this problem, predictions using the SGS clutter model are compared to established correlations taken from the porous media literature. The second class of problems is a cylinder in cross-flow for which both detailed experimental measurements and detailed CFD calculations of velocity deficit and kinetic energy profiles are available. Preliminary results indicate that this modeling approach offers a promising new approach to capture the macroscopic effects of small-scale objects without using excessive mesh resolution.

* Sandia is a multiprogram laboratory operated by Sandia Corporation, a Lockheed Martin Company, for the United States Department of Energy under Contract DE-AC04-94-AL85000.



## Introduction

Capturing object features using a CFD grid that are smaller than one one-hundredth the size of the computational domain requires an excessively large number of grid points and extremely small time steps for numerical integration. Relevant applications include large-scale problems such as forest fires down to smaller scale phenomena such as heat transfer in a porous media. An alternative approach to resolving these features is to use a subgrid scale (SGS) model to represent the macroscopic effects of these small features using reasonably sized CFD grid cells. The focus of this research is to develop engineering SGS models of flow transport in cluttered environments. This work is being carried out in a joint, iterative computational/experimental approach for which detailed experimental and CFD predictions are used to develop macroscopic models of clutter.

Subgrid clutter has two main physical effects on the macroscopic flow field. The first is to provide a momentum sink due to viscous and pressure drag forces of gas flowing through clutter. The second is to either increase or decrease the turbulent kinetic energy levels depending on the local clutter size, $l_c$, relative to the characteristic length scale of turbulence, $l_T$. In a qualitative sense, if $l_c < l_T$ the turbulent kinetic energy will decrease and if $l_c > l_T$ the turbulent kinetic energy will increase.

Previous investigations of turbulent flow in porous media can be found in previous studies of Pedras *et al.*[1,2,3], Nakayama *et al.*[4,5] and Antohe *et al.*[6]. In these

studies, time and phase-averaged transport equations of momentum, turbulent kinetic energy and turbulent dissipation rate are derived and constitutive models suggested for accounting for unknown SGS correlations and surface integral terms. These constitutive models are applicable to porous flow for which it is assumed that the characteristic size of the rigid porous matrix is much smaller than the size of the system [7]. This effort extends these approaches to clutter environments for which the length scale of the clutter is not necessarily small relative to the size of the system.

Discussion begins with first the mathematical formulation of the two-phase system based on the use of spatial filtering concepts. The filtering of the governing equations results in unknown correlations that require modeling. Constitutive models are formulated based on a linear combination of porous media and bluff body lift and drag relations. Results are then presented in support of the modeling assumptions and predictions of turbulent flow in porous media with comparisons to data from the literature. Experimental measurements of turbulent flow over a single cylinder are presented with comparisons to detailed CFD predictions. The information from the combined experimental and CFD predictions provide further calibration of the clutter model constants as part of future efforts in the clutter model development. Lastly, conclusions are drawn and future efforts are summarized.

## Mathematical Formulation of Two-Phase System

The following mathematical description is limited to a summary of the development of stationary clutter. The section starts with an introduction to the two-phase (*i.e.* spatial) averaging and time-averaging. The reasons for reviewing these mathematical formalities are to familiarize the reader with the concepts of spatial filtering and, more importantly, highlight the restrictions imposed by this approach with respect to the implementation of the clutter model into a CFD code. In the next section, these averaging concepts are applied to conservation equations for momentum, turbulent kinetic energy and dissipation transport. This averaging results in unknown second order correlations and surface integral terms that represent subgrid physics that must be closed with a clutter model. Requirements for the clutter model are provided based on both physical and computational requirements. The end result of this section is to provide a closed set of phase and time averaged transport equations for momentum, turbulent kinetic energy, and turbulent kinetic energy dissipation rate.

### Two-Phase Averaging

The formal averaging for two-phase media was first introduced by Anderson and Jackson[8] through the use of a local filtering function and later refined by Gray *et al.*[9] and Gough *et al.*[10] as presented in text book form by Kuo [11]. Alternatively, Slattery[12,13] offers a different derivation based on a spatially dependent volume of integration. The presentation here follows the procedure of Kuo. Figure 1 illustrates a typical phase averaging volume showing the total volume of interest, $V_T$, the volume of the solid clutter, $V_C$, and the volume of the gas, $V_g$.

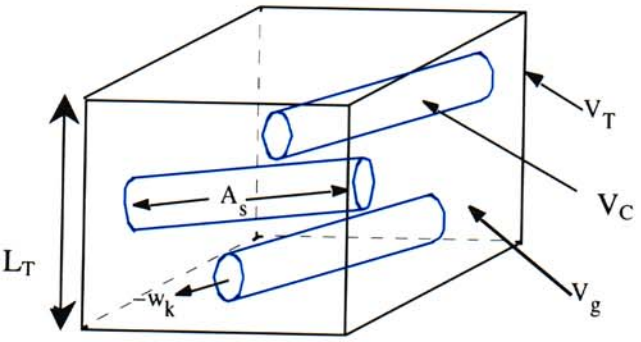


**Figure 1: Illustration of phase averaging volume.**

Phase averaged properties are obtained by first defining a spatial filtering function, $G\left[(x_i - x_i')/\Delta_f\right]$, with the normalization property: $\int_{V_\infty} G\left[(x_i - x_i')/\Delta_f\right]dV' = 1$.

For volume averaging using a cubic volume of length $L_T = (V_T)^{1/3}$ on a side then $\Delta_f = L_T$ and $G$ is defined as: $G = \frac{1}{V_T}\prod_{i=1}^{3}\left[H(x_i' - x_i + \Delta_f/2) - H(x_i' - x_i - \Delta_f/2)\right]$

where $H$ is the Heaviside function. Convoluting $G$ with the a gas property of interest, $\beta$, yields a gas phase average quantity,

$$\hat{\beta}(x_i) = \int_{V_{g_\infty}} \beta(x_i')G\left(\frac{x_i - x_i'}{\Delta_f}\right)dV' \qquad (1)$$

which physically represents a spatially averaged property over the volume, $V_T$. It should be emphasized that the volume of integration, $V_{g_\infty}$, represents all of the regions occupied by the gas and so does not depend on the location, $x_i$, where the averaging takes place. Of

more value is the intrinsic average, $\langle\beta\rangle$, defined as the local average of $\beta$ over the gas phase volume, $V_g$, for which constitutive and thermodynamic properties are well defined. The intrinsic average is defined as: $\langle\beta\rangle = \hat{\beta}/\phi$ and is the variable of interest to solve for after phase averaging the transport equations for mass, momentum and energy. The variable, $\phi$, is the void fraction and is defined as the volume of gas divided by the averaging volume, *i.e.* $\phi \equiv V_g/V_T = V_g/\Delta_f^3$.

**Temporal and Spatial Derivatives for Phase Averaging**

Applying the spatial filtering function to the transport equations requires expressing the phase averaged time and spatial partial derivatives in terms of temporal and spatial derivatives of phase averaged quantities. In the following development, the volume of the gas phase is assumed to change as a function of both time and space to accommodate for the complexities that may be included in future efforts (*e.g.* decomposing or burning clutter). Simplifications are then imposed to limit the scope to the focus of this work on turbulence modeling on rigid, stationary clutter.

**Time derivatives**

Relations for the temporal derivative are obtained by taking the partial derivative of $\hat{\beta}$.

$$\frac{\partial\hat{\beta}}{\partial t} = \frac{\partial}{\partial t}\int_{V_{g\infty}(t)} \beta(x_i')G\left(\frac{x_i - x_i'}{\Delta_f}\right)dV' \qquad (2)$$

Since the volume of the gas is assumed to be a function of time, Leibnitz rule[14] has to be applied to commute the temporal derivative term inside the volume averaging operator as follows:

$$\frac{\partial\hat{\beta}}{\partial t} = \int_{V_{g\infty}(t)} G\left(\frac{x_i - x_i'}{\Delta_f}\right)\frac{\partial\beta(x_i')}{\partial t}dV' + \int_{A_{g\infty}(t)} G\left(\frac{x_i - x_i'}{\Delta_f}\right)\beta(x_i')w_k(x_i')\,dA_k' \qquad (3)$$

In Eq. (3), the first term on the right hand size is simply the definition of the phase averaged time rate in change of $\beta$, *i.e.* $\widehat{\partial\beta/\partial t}$. The second term is a surface integral that accounts for material crossing the boundary of the phase averaging volume as a function of time where $w_k$ is the velocity of the surface (pointing into the solid clutter, see Figure 1) of the gas phase volume, $V_g$, on the surface, $A_g$. The gas phase surface can be further broken into the contribution associated with the clutter, $A_c$, and rest of the surface area associated with the phase averaging volume, $A_{g-c}$. Since $G$ goes to zero at the boundary on the surface $A_{g-c}$ then the contribution of the surface integral in those regions is equal to zero resulting in the following relation for the phase averaged time derivative.

$$\widehat{\frac{\partial\beta}{\partial t}} = \frac{\partial}{\partial t}\hat{\beta} - \int_{A_C(t)} G\left(\frac{x_i - x_i'}{\Delta_f}\right)\beta(x_i')w_k(x_i')\,dA_k' \qquad (4)$$

Assuming the clutter surface is rigid and non-porous then the normal velocity to the clutter surface is identically zero (*i.e.* $w_k = 0$) allowing for the temporal derivative to commute with the filter operation resulting in the simple relation.

$$\widehat{\frac{\partial\beta}{\partial t}} = \frac{\partial}{\partial t}\hat{\beta} \qquad (5)$$

**Space derivatives with uniform filter width** (*i.e.* $\Delta_f = const$)

Analogous to the development for time derivatives, a spatial derivative relation is obtained by taking the divergence of a phase-averaged vector quantity.

$$\frac{\partial}{\partial x_j}\hat{\beta}_j(x_i) = \frac{\partial}{\partial x_j}\int_{V_{g\infty}} \beta_j(x_i')G\left(\frac{x_i - x_i'}{\Delta_f}\right)dV' \qquad (6)$$

Since the volume averaging is independent of the location, the partial derivative can be brought inside the integration and applied directly to the filtering function $G$.

$$\frac{\partial}{\partial x_j}\hat{\beta}_j(x_i) = \int_{V_{g\infty}} \beta_j(x_i')\frac{\partial}{\partial x_j}G\left(\frac{x_i - x_i'}{\Delta_f}\right)dV' \qquad (7)$$

For uniform filter size (*i.e.* $\Delta_f = const$), then $\partial G/\partial x_j = -\partial G/\partial x_j'$ and using the chain rule of differentiation then Eq. (7) can be expressed as:

$$\frac{\partial}{\partial x_j}\hat{\beta}_j(x_i) = \int_{V_c} \left\{ G\left(\frac{x_i - x_i'}{\Delta_f}\right)\frac{\partial \beta_j(x_i')}{\partial x_j'} - \frac{\partial}{\partial x_j'}\left[\beta_j(x_i')G\left(\frac{x_i - x_i'}{\Delta_f}\right)\right]\right\} dV' \quad . \quad (8)$$

The first term on the right hand size of Eq. (8) is the two-phase average of the gradient of the vector quantity and the second term can be further expressed in terms of a surface integral using the divergence theorem. Rearranging terms leads to an expression for the phase averaged divergence of a vector quantity in terms of the divergence of a phase averaged quantity and a surface integral to account for microscopic clutter effects.

$$\widehat{\frac{\partial \beta_j(x_i)}{\partial x_j}} = \frac{\partial \hat{\beta}_j(x_i)}{\partial x_j} + \int_{A_c} G\left(\frac{x_i - x_i'}{\Delta_f}\right)\beta_j(x_i')dA_j' \quad (9)$$

An important assumption in the derivation of Eq. (9) is ***the filter width is assumed to be constant.*** That is, the filter width is assumed to be invariant with space and time. Alternatively, the development of a non-uniform filter width could be pursued for which $\partial G/\partial x_j \neq -\partial G/\partial x_j'$. However, the introduction of such a filter introduces commutation error that has been discussed in the Large Eddy Simulation (LES) literature[15,16,17] as well as an extra surface integral error term[18]. The former of these two sources of error has been somewhat mitigated using filter functions that satisfy commutivity up to some order of accuracy[17]. However, the second source of error is more difficult to treat and leads to a violation of mass, momentum and energy conservation when these quantities are exchanged between phases[18]. These issues affect practical application. Often the filter width is assumed to be proportional to the local grid size, *e.g.* $\Delta_f = C\,\Delta_x$, where $\Delta_x$ is the local grid cell size and $C$ is a constant that is greater or equal to one. Therefore in a practical engineering problem where the CFD grid cell size changes in space, then the assumption of $\Delta_f = const$ is violated! In order to avoid this contradiction, ***the filter width is assumed to be independent from the grid.*** This choice also has the added benefit to allowing for grid convergence (see requirement 4 of the following discussion). The disadvantages of a filter width that is independent of the grid are two fold. First the clutter model must be able to capture the relevant physics over a wide range of filter to clutter size ratios (see requirement 1 of the following discussion). Secondly, the coding of the clutter model is further complicated with the introduction of an integral of the clutter source terms to account for the effects of intermittency (see requirement 3 of below discussion).

Thus far, only phase averaging concepts have been briefly reviewed. In addition, it is also desirable to time average the governing equations of mass, momentum and energy transport. Time averaging removes any remaining high frequency turbulence signal and is compatible with the Reynolds Averaged Navier Stokes (RANS) transport equations that are commonly used for solving practical engineering applications. Time averaging issues are not reviewed in this paper but can be found in several excellent introductory texts on turbulence[19,20].

## Phase and Time Averaged Transport Equations

Applying the phase averaging relations given by Eqs. (5) and (9), in addition to time averaging, to the transport equations of momentum, turbulent kinetic energy and turbulent dissipation results in a set of phase-and-time averaged transport equations containing unknown second order correlations and surface integral terms. Both of these terms require explicit subgrid scale modeling. In order to develop models for these terms, a set of guiding principals are employed.

### Guiding Principals for Clutter Subgrid Scale Model

The following four principals provide guidance for the development of the SGS clutter model. These requirements are summarized below with a diagram illustrating each constraint for a two-dimensional domain.

1. **The clutter model(s) should be able to accommodate a spectrum of clutter sizes ranging from a single object (*i.e.* bluff body drag) to many objects that are randomly placed (*i.e.* clutter that resembles porous media) since the filter width of the phase averaging is assumed to be constant.**

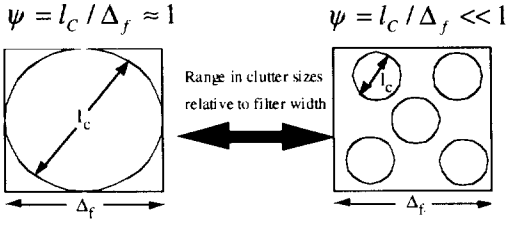

**2. The clutter model(s) should provide a mechanism to represent isotropic (*i.e.* rotationally invariant) as well as anisotropic (rotationally dependent) clutter with minimal amount of user input.**

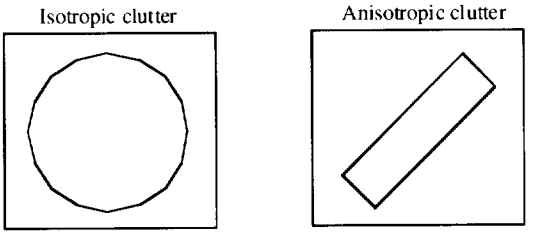


**3. The clutter model(s) should allow for intermittency within the filtering volume so that non-periodic SGS clutter may be addressed.**

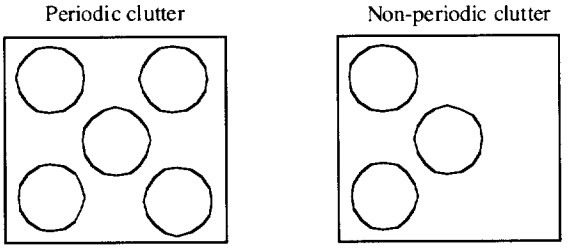


**4. The clutter model(s) should allow for grid convergence studies to be performed. This implies that the numerical grid should be chosen independent of the phase averaging filtering volume.**

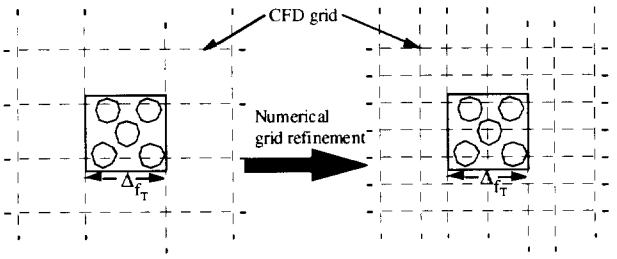


Imposing these constraints guide the final form for the closure terms needed for the phase and time averaged transport equations. The descriptions of these models are broken into two classes of clutter models. The first is the isotropic class where the clutter is treated as a collection of spheres. The second is the anisotropic class for which the clutter is treated as a collection of cylinders.

## Conservation of Linear Momentum

Phase and time averaging the Navier-Stokes equations for momentum transport and assuming constant density and molecular viscosity results in the following,

$$\rho\left[\frac{\partial}{\partial t}\left(\phi\langle\overline{u}_j\rangle\right)+\frac{\partial}{\partial x_i}\left(\phi\langle\overline{u}_i\rangle\langle\overline{u}_j\rangle\right)\right]= -\frac{\partial\left(\phi\langle\overline{p}\rangle\right)}{\partial x_i}+\frac{\partial\phi\langle\overline{\tau}_{ij}\rangle}{\partial x_i}-\frac{\partial\left[\phi\left(\langle\overline{u}_i\rangle\langle\overline{u}_j\rangle-\langle\overline{u_iu_j}\rangle\right)\right]}{\partial x_i} -\int_{A_i}\left[\overline{p}\delta_{ij}-\overline{\tau}_{ij}\right]dA_i' \tag{10}$$

where the $\langle\overline{\ldots}\rangle$ notation refers to a time-and-phase averaged quantity. The term $\langle\overline{u}_i\rangle\langle\overline{u}_j\rangle-\langle\overline{u_iu_j}\rangle$ represents the effects of the subgrid fluctuations in time and space and can be decomposed into three terms using the double decomposition approach of Pedras *et al.*[3]. This term physically represents the effects of i) turbulent Reynolds stresses due to macroscopic phase averaged velocity, ii) dispersion due to spatial fluctuations of macroscopic time averaged velocity and iii) dispersion due to microscopic time averaged velocity. The first two of these effects are modeled using a turbulent eddy viscosity[19] and Brinkman[21,22] models, respectively. The dispersion of momentum due to microscopic time-averaged velocity is simply neglected due for lack of an established model. The closure for the surface integral term is based on a linear weighting of constitutive models from the porous media literature[1-7] and simple bluff body lift and drag models[23,24]. A weighting function, $\psi$, is defined as the ratio of the length scale of the clutter to the size of the filtering volume, *i.e.* $\psi=l_C/\Delta_f$, and is used to develop a modeled transport equation for Eq. (10) as follows.

$$\rho\left[\frac{\partial}{\partial t}\left(\phi\langle\overline{u}_j\rangle\right)+\frac{\partial}{\partial x_i}\left(\phi\langle\overline{u}_i\rangle\langle\overline{u}_j\rangle\right)\right] +\frac{\partial\left(\phi\langle\overline{p}\rangle\right)}{\partial x_i}-\frac{\partial\left[\phi\tau_{ij}\left(\langle\overline{u}_i\rangle,\langle\overline{u}_j\rangle\right)\right]}{\partial x_i}= +\frac{\partial}{\partial x_i}\left[\phi\left(\mu_T+(1-\psi)\mu_B\right)\left(\frac{\partial\langle\overline{u}_j\rangle}{\partial x_i}+\frac{\partial\langle\overline{u}_i\rangle}{\partial x_j}\right)\right] -\frac{1}{\Delta^3{}_f}\int_{V_T}\left[(1-\psi)S_{P_j}+\psi S_{B_j}\right]GdV \tag{11}$$

The first term on the right hand side of Eq. (11) are models to represent the effects of microscopic

dispersion and turbulent fluctuations using Brinkman[21,22], $\mu_B$, and turbulent eddy[19], $\mu_T$, viscosity models, respectively. The source terms, $S_{P_j}$ and $S_{B_j}$, represent the gas phase exchange at the surface of the solid for the limits of a porous media and bluff body drag, respectively. The exact functional form of these terms will be discussed shortly for the isotropic and anisotropic clutter classes. These two source terms are blended depending on the size of the clutter relative to the filtering volume. Recall, this blending is employed to satisfy first constraint condition for of the clutter model formulation previously defined. The linear weighting used is not unique and other weightings could have been chosen. An example of using a linear blending of constitutive models for the isotropic clutter class is presented in the results to assess the utility of this approach. In addition to the blending, these source terms are also averaged over the filtering volume. The motivation for introducing this averaging is to satisfy the third constraint condition for the clutter model to account for non-periodic clutter.

### *Isotropic Clutter Class*

The first type of clutter class considered is for isotropic media that is represented by a collection of spheres. Spheres are chosen to represent this class due to the abundant amount of drag data available in the literature over a wide range of Reynolds numbers. For this class, the effects of the clutter are modeled as a combination of a modified Darcy-Forchheimer Law for porous media[25] and a bluff body drag relations for the linear superposition of a collection of spheres.

$$S_{P_j} = \phi^2 \langle \overline{u}_j \rangle \left[ \mu / K + C_2 \phi \rho \left| \langle \overline{u}_k \rangle \right| / \sqrt{K} \right] \qquad (12)$$

$$S_{B_j} = (2/3)\rho \left| \langle \overline{u}_k \rangle \right| \langle \overline{u}_j \rangle (1-\phi) C_D / D \qquad (13)$$

In Eq. (12), $K \left( \equiv -\mu \phi \langle u_j \rangle / (\partial p / \partial x_j) \right)$ is defined as the permeability and is determined using the empirical relation $K = \phi^3 D^2 / \left[ C_1 (1-\phi)^2 \right]$ where $C_1$ is set equal to 147 based on the work of Kuwahara *et al.* [5]. The value of $C_2$ is set to either 1.75 as suggested by Kuwahara *et al.*[5] or to 2.3 based on the classical result of Ergun[26]. Calculations presented in the results shows that the total drag from a collection of spheres shows the overall drag is not sensitive to the value of $C_2$. In the bluff body limit, the clutter is treated as a collection of spheres for which the total number of spheres in the filtering volume can be related to porosity and ratio of clutter to filtering size using the relation: $N_S = 6(1-\phi)(D/\Delta_f)^3/\pi$. In Eq. (13), $C_D$ is the coefficient of drag of each sphere given by the following empirical relation.

$$C_D = \begin{cases} 24\left(1 + \mathrm{Re}_D^{2/3}/6\right)/\mathrm{Re}_D & \text{for } \mathrm{Re}_D \le 1000 \\ 0.424 & \text{for } \mathrm{Re}_D > 1000 \end{cases} \qquad (14)$$

### *Anisotropic Clutter Class*

In order to satisfy the second constraint for the clutter model, an anisotropic clutter class is addressed. The orientation of the flow relative to the clutter will greatly affect the drag due to the change in projected area as well as any lift force components that are normal to the flow direction. The geometry chosen to represent the anisotropic clutter class is a collection of cylinders for which the force on each cylinder can be decomposed into directions along the length of cylinder, $\hat{e}_{\parallel}$, and normal to cylinder, $\hat{e}_{\perp 1}$ and $\hat{e}_{\perp 2}$, as illustrated Figure 2.

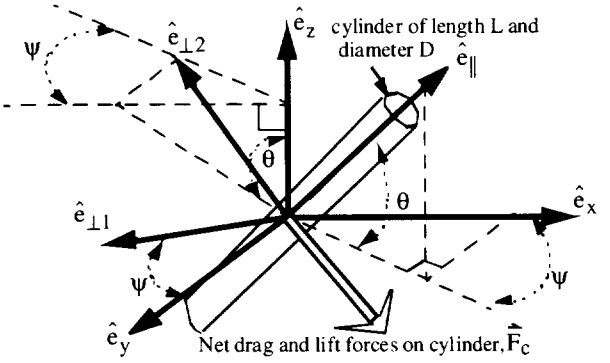


**Figure 2: Decomposition of net force using a coordinate system attached to the cylinder and a fixed Cartesian coordinate system.**

The relationship between the transformed coordinate system, $(\hat{e}_{\parallel}, \hat{e}_{\perp 1}, \hat{e}_{\perp 2})$, and the fixed Cartesian coordinate system, $(\hat{e}_x, \hat{e}_y, \hat{e}_z)$, is given by following rotation of basis coordinate transformation,

$$\begin{Bmatrix} \hat{e}_{\parallel} \\ \hat{e}_{\perp 1} \\ \hat{e}_{\perp 2} \end{Bmatrix} = \underline{\underline{T}} \begin{Bmatrix} \hat{e}_x \\ \hat{e}_Y \\ \hat{e}_Z \end{Bmatrix} = \begin{bmatrix} \cos\theta\cos\psi & \cos\theta\sin\psi & \sin\theta \\ -\sin\psi & \cos\psi & 0 \\ -\sin\theta\cos\psi & -\sin\theta\sin\psi & \cos\theta \end{bmatrix} \begin{Bmatrix} \hat{e}_x \\ \hat{e}_Y \\ \hat{e}_Z \end{Bmatrix} \qquad (15)$$

where the direction angles $\theta$ and $\psi$ are defined using the following relations.

$$\sin\delta = \hat{e}_{\|} \bullet \hat{e}_Z$$
$$\cos\theta\sin\psi = \hat{e}_{\|} \bullet \hat{e}_Y \quad (16)$$
$$\cos\theta\cos\psi = \hat{e}_{\|} \bullet \hat{e}_Z$$

In the porous media limit, the modified Darcy-Forchheimer Law is again used except now the permeability is expressed in terms of a second order tensor resulting in the following expression for $S_{P_j}$.

$$S_{P_j} = \phi^2\left[\langle\overline{\mu}\rangle K_{jp}^{-1} + \rho C_2\phi\left|\langle\overline{u}_k\rangle\right|\left(\sqrt{K_{jp}}\right)^{-1}\right]\langle\overline{u}_p\rangle \quad (17)$$

If the clutter is assumed to be orthotropic then the permeability tensor can be expressed in terms of a permeability components aligned with the cylinders, $K_{\|}$, and components perpendicular to the cylinder, $K_{\perp 1}$ and $K_{\perp 2}$ in the $(\hat{e}_{\|}, \hat{e}_{\perp 1}, \hat{e}_{\perp 2})$ coordinate system.

$$\underline{\underline{K}}^*(\hat{e}_{\|}, \hat{e}_{\perp 1}, \hat{e}_{\perp 2}) = \begin{bmatrix} K_{\|} & 0 & 0 \\ 0 & K_{\perp 1} & 0 \\ 0 & 0 & K_{\perp 2} \end{bmatrix} \quad (18)$$

These coordinate directions represent the principal directions of the permeability tensor. The superscript * denotes that the tensor should be applied to a velocity field expressed in terms of the $(\hat{e}_{\|}, \hat{e}_{\perp 1}, \hat{e}_{\perp 2})$ coordinate system. The empirically based models for $K_{\perp 1}$ and $K_{\perp 2}$ are same as used in Eq. (12),

$$K_{\perp 1} = K_{\perp 2} = \phi^3 D^2 / \left[C_1(1-\phi)^2\right] \quad (19)$$

while the relation for $K_{\|}$ comes from the use of Carman-Kozey theory for flow along an array of cylinders [7].

$$K_{\|} = \frac{D^2}{32(1-\phi)}\left[2\ln(1/(1-\phi)) - 3 + 4(1-\phi) - (1-\phi)^2\right] \quad (20)$$

In order to make use of the permeability tensor in a calculation it must be expressed in terms of a Cartesian coordinate system using the following transformation,

$$\underline{\underline{K}} = \underline{\underline{T}}^{-1}\,\underline{\underline{K}}^*\,\underline{\underline{T}} \quad (21)$$

where $\underline{\underline{T}}$ is defined in Eq. (15) and $\underline{\underline{T}}^{-1} = \underline{\underline{T}}^T$ since $\underline{\underline{T}}$ is a unitary matrix. Carrying out the matrix multiplication in Eq. (21) results in the following for $K_{pj}^{-1}$ from Eq. (17),

$$K_{pj}^{-1} = \begin{bmatrix} K_{11}^{-1} & K_{12}^{-1} & K_{13}^{-1} \\ K_{21}^{-1} & K_{22}^{-1} & K_{23}^{-1} \\ K_{31}^{-1} & K_{32}^{-1} & K_{33}^{-1} \end{bmatrix}$$

where,

$$K_{11}^{-1} = \frac{(\sin\psi)^2}{K_{\perp 1}} + (\cos\psi)^2\left[\frac{(\cos\theta)^2}{K_{\|}} + \frac{(\sin\theta)^2}{K_{\perp 2}}\right]$$
$$K_{22}^{-1} = \frac{(\cos\psi)^2}{K_{\perp 1}} + (\sin\psi)^2\left[\frac{(\cos\theta)^2}{K_{\|}} + \frac{(\sin\theta)^2}{K_{\perp 2}}\right]$$
$$K_{33}^{-1} = \frac{(\cos\theta)^2}{K_{\perp 2}} + \frac{(\sin\theta)^2}{K_{\|}} \quad (22)$$
$$K_{21}^{-1} = K_{12}^{-1} = \cos\psi\sin\psi\left[\frac{(\cos\theta)^2}{K_{\|}} + \frac{(\sin\theta)^2}{K_{\perp 2}} - \frac{1}{K_{\perp 1}}\right]$$
$$K_{31}^{-1} = K_{13}^{-1} = \cos\psi\sin\theta\cos\theta\left[\frac{1}{K_{\|}} - \frac{1}{K_{\perp 2}}\right]$$
$$K_{23}^{-1} = K_{32}^{-1} = \sin\psi\sin\theta\cos\theta\left[\frac{1}{K_{\|}} - \frac{1}{K_{\perp 2}}\right]$$

For anisotropic clutter class in the limit of bluff body drag, empirical correlations for the coefficient of lift and drag are available in the handbook by Blevins[23] for long cylinders at an incline as illustrated in the sketch below.

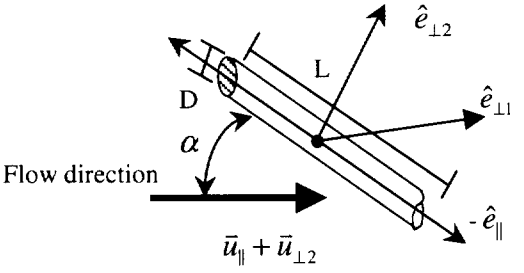


Coefficient of lift and drag for tangential force:

$$C_{\|} \approx 0.083\cos\alpha - 0.035\cos^2\alpha$$

Coefficient of lift and drag for normal force:

$$C_{\perp 2} \approx 1.2\sin^2\alpha$$

**Figure 3: Sketch of inclined cylinder and lift and drag correlations from Blevins [23].**

Note, that the relations for lift and drag in Fig. 3 are only valid under the conditions that there is no cross

flow. Approximations have to be introduced for cylinders exposed to an arbitrary orientation relative to the mean flow. This need is addressed by assuming that the total force on the cylinder, $\vec{F}_C$, is the result of the superposition of the lift and drag along and normal to the cylinder, shown in Fig. 3, in addition to a drag force from gas flowing across the cylinder for which $C_{\perp 1}$ is set to a value of 1.2. Making these approximations, the total net force on the cylinder may be expressed as:

$$\begin{aligned}\vec{F}_C &= \vec{F}_{C_\parallel} + \vec{F}_{C_{\perp 1}} + \vec{F}_{C_{\perp 2}} \\ &= \frac{\langle\overline{\rho}\rangle C_\parallel A_\parallel}{2}\left|\langle\overline{\vec{u}}_\parallel\rangle + \langle\overline{\vec{u}}_{\perp 2}\rangle\right|^2 \langle\overline{\vec{u}}_\parallel\rangle / \left|\langle\overline{\vec{u}}_\parallel\rangle\right| \\ &+ \frac{\langle\overline{\rho}\rangle C_{\perp 1} A_{\perp 1}}{2}\left|\langle\overline{\vec{u}}_{\perp 1}\rangle\right|\langle\overline{\vec{u}}_{\perp 1}\rangle \\ &+ \frac{\langle\overline{\rho}\rangle C_{\perp 2} A_{\perp 2}}{2}\left|\langle\overline{\vec{u}}_\parallel\rangle + \langle\overline{\vec{u}}_{\perp 2}\rangle\right|^2 \langle\overline{\vec{u}}_{\perp 2}\rangle / \left|\langle\overline{\vec{u}}_{\perp 2}\rangle\right|\end{aligned} \tag{23}$$

where $A_\parallel$, $A_{\perp 1}$ and $A_{\perp 2}$ are the reference (projected) areas of the cylinder and are equal to $\pi DL$, $DL$ and $DL$, respectively. The net force on the cylinder or group of cylinders is related to the momentum source term, $\vec{S}_B$, of Eq. (11) using the relation,

$$\vec{S}_B = N_C \vec{F}_C / \Delta_f^{\,3} \tag{24}$$

where $N_C$ is the total number of cylinders that are prescribed within the filtering volume.

In order to determine these forces, the angle $\alpha$ is required for the coefficients of lift and drag and is obtained using the relation:

$$\alpha = \cos^{-1}\left(\frac{\langle\overline{\vec{u}}_\parallel\rangle \bullet \left(\langle\overline{\vec{u}}_\parallel\rangle + \langle\overline{\vec{u}}_{\perp 2}\rangle\right)}{\left|\langle\overline{\vec{u}}_\parallel\rangle\right|\left|\langle\overline{\vec{u}}_\parallel\rangle + \langle\overline{\vec{u}}_{\perp 2}\rangle\right|}\right) \tag{25}$$

where $\langle\overline{\vec{u}}_\parallel\rangle$, $\langle\overline{\vec{u}}_{\perp 1}\rangle$ and $\langle\overline{\vec{u}}_{\perp 2}\rangle$ are the components of the time and phase-averaged velocity in the $(\hat{e}_\parallel, \hat{e}_{\perp 1}, \hat{e}_{\perp 2})$ coordinate system have the following definitions.

$$\begin{aligned}\langle\overline{\vec{u}}_\parallel\rangle &= u_\parallel \hat{e}_\parallel \\ \langle\overline{\vec{u}}_{\perp 1}\rangle &= u_{\perp 1}\hat{e}_{\perp 1} \\ \langle\overline{\vec{u}}_{\perp 2}\rangle &= u_{\perp 2}\hat{e}_{\perp 2}\end{aligned} \tag{26}$$

The magnitudes of the velocities in Eq. (26) can be expressed in terms of velocity components in a Cartesian coordinate system using the transformation.

$$\begin{Bmatrix} u_\parallel \\ u_{\perp 1} \\ u_{\perp 2}\end{Bmatrix} = \underline{\underline{T}}\begin{Bmatrix} u \\ v \\ w\end{Bmatrix} = \begin{bmatrix} \cos\theta\cos\psi & \cos\theta\sin\psi & \sin\theta \\ -\sin\psi & \cos\psi & 0 \\ -\sin\theta\cos\psi & -\sin\theta\sin\psi & \cos\theta\end{bmatrix}\begin{Bmatrix} u \\ v \\ w\end{Bmatrix} \tag{27}$$

Substituting Eqs. (26) and (27) into Eq. (25) and after significant algebraic manipulation then $\alpha$ can be expressed in terms of known scalar velocities, $u$, $v$, $w$ and the angles $\theta$ and $\psi$.

$$\alpha = \cos^{-1}\left(\alpha_{num} / \alpha_{denom}\right) \tag{28}$$

where,

$$\alpha_{num} = \left|u\left[\cos(\psi-\theta)+\cos(\psi+\theta)\right] + v\left[\sin(\psi-\theta)+\sin(\psi+\theta)\right] + 2w\sin\theta\right|$$

and

$$\alpha_{denom} = \left\{2\left[u^2+v^2+2w^2+\left(u^2-v^2\right)\cos(2\psi)+2uv\sin(2\psi)\right]\right\}^{1/2}.$$

In obtaining the numerator and denominator of Eq. (28), the magnitude of the various velocity components and sums of components expressed in terms of a Cartesian coordinate system is required. These terms are summarized below for completeness.

$$\begin{aligned}\left|\langle\overline{\vec{u}}_\parallel\rangle\right| = |\,&u\left[\cos(\psi-\theta)+\cos(\psi+\theta)\right] \\ &+ v\left[\sin(\psi-\theta)+\sin(\psi+\theta)\right] \\ &+ 2w\sin\theta\,)\,|\,/\,2\end{aligned} \tag{29}$$

$$\left|\langle\overline{\vec{u}}_{\perp 1}\rangle\right| = \left|v\cos\psi - u\sin\psi\right| \tag{30}$$

$$\begin{aligned}\left|\langle\overline{\vec{u}}_{\perp 2}\rangle\right| = |\,&u\left[\sin(\psi-\theta)-\sin(\psi+\theta)\right] \\ &+ v\left[\cos(\psi+\theta)-\cos(\psi-\theta)\right] \\ &+ 2w\cos\theta\,)\,|\,/\,2\end{aligned} \tag{31}$$

$$\begin{aligned}\left|\langle\overline{\vec{u}}_{\perp 1}\rangle + \langle\overline{\vec{u}}_{\perp 2}\rangle\right| = \Big\{&\left[u^2+v^2+2w^2\right) \\ &+\left(u^2-v^2\right)\cos(2\psi)+2uv\sin(2\psi)\Big]/2\Big\}^{1/2}\end{aligned} \tag{32}$$

Once $\vec{F}_C$ is calculated then the source term $\vec{S}_B$ is determined using Eq. (24) and summarized below for a Cartesian coordinate system.

$$
\begin{aligned}
S_{B_x} &= \frac{N_C \vec{F}_C \bullet \hat{e}_x}{\Delta_f^{\,3}} = \frac{N_C \rho}{2\Delta_f^{\,3}}\Big[ C_{\parallel} A_{\parallel} \left|\langle \bar{u}_{\parallel} \rangle\right| + \langle \bar{u}_{\perp 2} \rangle \Big|^2 / \left|\langle \bar{u}_{\parallel} \rangle\right| \\
&\{\cos\theta\cos\psi[u\cos\theta\cos\psi + v\cos\theta\sin\psi + w\sin\theta]\} \\
&+ C_{\perp 2} A_{\perp 2} \left|\langle \bar{u}_{\parallel} \rangle + \langle \bar{u}_{\perp 2} \rangle\right|^2 / \left|\langle \bar{u}_{\perp 2} \rangle\right| \\
&\{\sin\theta\cos\psi[u\sin\theta\cos\psi + v\sin\theta\sin\psi - w\cos\theta]\} \\
&+ C_{\perp 1} A_{\perp 1} \left|\langle \bar{u}_{\perp 1} \rangle\right| \{\sin\psi[u\sin\psi - v\cos\psi]\}\Big]
\end{aligned}
\tag{33}
$$

$$
\begin{aligned}
S_{B_Y} &= \frac{N_C \vec{F}_C \bullet \hat{e}_Y}{\Delta_f^{\,3}} = \frac{N_C \rho}{2\Delta_f^{\,3}}\Big[ C_{\parallel} A_{\parallel} \left|\langle \bar{u}_{\parallel} \rangle\right| + \langle \bar{u}_{\perp 2} \rangle \Big|^2 / \left|\langle \bar{u}_{\parallel} \rangle\right| \\
&\{\cos\theta\sin\psi[u\cos\theta\cos\psi + v\cos\theta\sin\psi + w\sin\theta]\} \\
&+ C_{\perp 2} A_{\perp 2} \left|\langle \bar{u}_{\parallel} \rangle + \langle \bar{u}_{\perp 2} \rangle\right|^2 / \left|\langle \bar{u}_{\perp 2} \rangle\right| \\
&\{\sin\theta\sin\psi[u\sin\theta\cos\psi + v\sin\theta\sin\psi - w\cos\theta]\} \\
&+ C_{\perp 1} A_{\perp 1} \left|\langle \bar{u}_{\perp 1} \rangle\right| \{-\cos\psi[u\sin\psi - v\cos\psi]\}\Big]
\end{aligned}
\tag{34}
$$

$$
\begin{aligned}
S_{B_Z} &= \frac{N_C \vec{F}_C \bullet \hat{e}_Z}{\Delta_f^{\,3}} = \frac{N_C \rho}{2\Delta_f^{\,3}}\Big[ C_{\parallel} A_{\parallel} \left|\langle \bar{u}_{\parallel} \rangle\right| + \langle \bar{u}_{\perp 2} \rangle \Big|^2 / \left|\langle \bar{u}_{\parallel} \rangle\right| \\
&\{\sin\theta[u\cos\theta\cos\psi + v\cos\theta\sin\psi + w\sin\theta]\} \\
&+ C_{\perp 2} A_{\perp 2} \left|\langle \bar{u}_{\parallel} \rangle + \langle \bar{u}_{\perp 2} \rangle\right|^2 / \left|\langle \bar{u}_{\perp 2} \rangle\right| \\
&\{\cos\theta[u\sin\theta\cos\psi + v\sin\theta\sin\psi - w\cos\theta]\}\Big]
\end{aligned}
\tag{35}
$$

**Conservation of Turbulent Kinetic Energy and Dissipation Rate**

Details on the derivation of the phase averaged k and ε equations can be found in Ref. [1] and the modeled form of them are summarized below for use with the clutter model.

$$
\begin{aligned}
&\rho\left[\frac{\partial}{\partial t}\left(\phi\langle k\rangle\right) + \frac{\partial}{\partial x_i}\left(\phi\langle \bar{u}_i\rangle\langle k\rangle\right)\right] = \\
&\frac{\partial}{\partial x_i}\left[\left(\mu + \mu_T\right)\frac{\partial}{\partial x_i}\left(\phi\langle k\rangle\right)\right] \\
&- \rho\phi\left\langle \overline{u_i' u_j'}\right\rangle \frac{\partial\left(\phi\langle \bar{u}_j\rangle\right)}{\partial x_i} - \rho\phi\langle\varepsilon\rangle \\
&+ \frac{1}{\Delta_f^{\,3}}\int_{V_T}\langle k\rangle\left(C_{k_P} S_{P_j} + C_{k_B} S_{B_j}\right)/\left(\phi\langle \bar{u}_j\rangle\right) G\, dV
\end{aligned}
\tag{36}
$$

$$
\begin{aligned}
&\rho\left[\frac{\partial}{\partial t}\left(\phi\langle\varepsilon\rangle\right) + \frac{\partial}{\partial x_i}\left(\phi\langle \bar{u}_i\rangle\langle\varepsilon\rangle\right)\right] = \frac{\partial}{\partial x_i}\left[\left(\mu + \mu_T\right)\frac{\partial}{\partial x_i}\left(\phi\langle\varepsilon\rangle\right)\right] \\
&- C_{\varepsilon 1}\rho\left\langle \overline{u_i' u_j'}\right\rangle \frac{\partial\left(\phi\langle \bar{u}_j\rangle\right)}{\partial x_i}\frac{\langle\varepsilon\rangle}{\langle k\rangle} - C_{\varepsilon 2}\rho\phi\frac{\langle\varepsilon\rangle^2}{\langle k\rangle} \\
&+ \frac{1}{\Delta_f^{\,3}}\int_{V_T} C_{\varepsilon 2}\rho\langle\varepsilon\rangle\left\{C_{k_P} S_{P_j} + C_{k_B} S_{B_j}\right\} G/\left(\phi\langle \bar{u}_j\rangle\right) dV
\end{aligned}
\tag{37}
$$

The unique feature of the closed modeled terms in Eqs. (36) and (37) is again the use of the averaged source terms over the filtering volume to account for the effects of non-periodic clutter. The constants $C_{k_P}$ and $C_{k_B}$ require calibration for the limits of porous media and bluff body drag, respectively. The constant associated with the porous media limit, $C_{k_P}$, is set to a value of 0.28 to be consistent with the results of Pedras *et al.* [1]. The second constant, $C_{k_B}$, will eventually be set based on the results of detailed measurements and CFD predictions, to be discussed in the results section.

## Numerical Implementation

The clutter models discussed in the previous section are implemented into a general-purpose fire simulation code, VULCAN, which is based on the KAMELEON-Fire code[27]. VULCAN uses a RANS based model suite including a k-ε turbulence model[28]. Numerical discretization is on a staggered, block-structured grid with second-order upwind differencing for the convective terms using a version of the SIMPLE algorithm[29]. Previous studies have included using VULCAN for pool fire simulations[30,31]. The source terms appearing in Eqs. (12), (13), (17) and (33)-(35) for momentum transport are treated in a semi-implicit nature to maintain numerical stability. The source terms appearing in Eqs. (36) (36)and (37) are implemented in an explicit manner.

## Results

### *Assessment of Linear Blending of $\vec{S}_P$ and $\vec{S}_B$ Assumption*

An assessment of using a linear blending of constitutive models from the porous media and bluff body drag is investigated for a collection of spheres where the clutter is considered isotropic. Figure 4 (a) and (b) show results of the drag force per unit volume using a modified Darcy-Forchheimer Law and also a bluff body

drag relations using Eqs. (12) and (13), respectively. The results show that the porous media and bluff body drag have a similar functional dependence on Reynolds number with the two predicting almost the same force per unit volume for either low porosity at high Reynolds number or for high porosity at low Reynolds number. This suggests that the linear blending of these two limits is a reasonable approach to span the possible range of clutter sizes for the isotropic clutter class. Further work is required to see if the same approach is also appropriate for the anisotropic clutter.

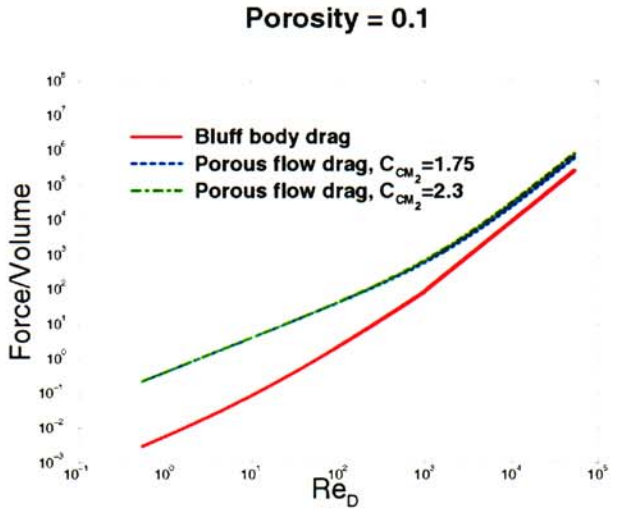


(a)

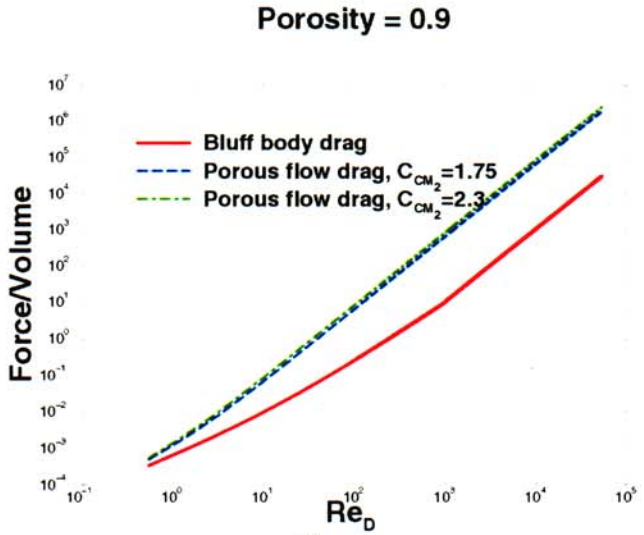


(b)

**Figure 4: Force/volume using constitutive models for a collection of spheres from porous media and bluff body drag relations using a porosity of (a) 0.1 and (b) 0.9.**

*Verification of Anisotropic Clutter Class for Single Cylinder in a Cross Flow*

The anisotropic clutter class is developed based on empirical relations from Blevins[23] for lift and drag on an inclined cylinder from the relations normal and aligned to a cylinder shown in Figure 3. In the limiting case of $v = w = 0$, $u = -U_\infty$, $\psi = 0$ and $\delta = \alpha$ then the drag and lift force in Eqs. (33) and (35) may be directly compared with the result from Hoerner[24] for drag and lift on a cylinder at an angle of attack equal to $\alpha$, illustrated in the sketch below.

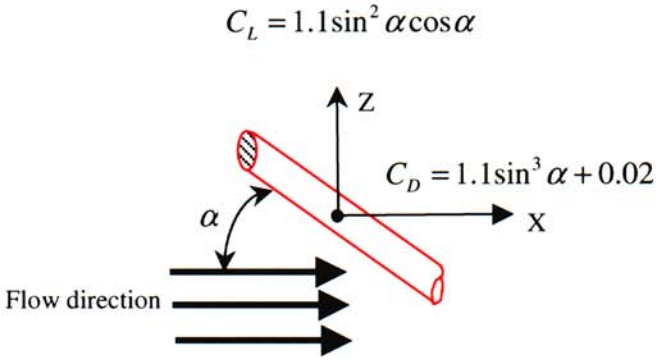


**Figure 5: Sketch of cylinder at angle of attack, α, and coefficients of lift and drag from Hoerner [24].**

Substituting in the drag and lift relations from Figure 3 into Eqs. (33) and (35) for this case results in the following for $\vec{F}_C$.

$$\vec{F}_C = \frac{-\rho U_\infty^{\,2}}{2}\left[\left\{A_{\perp 2}\left[1.2\sin^3\alpha\right] + A_{\parallel}\left[0.083\cos^2\alpha - 0.035\cos^3\alpha\right]\right\}\hat{e}_X + \left\{A_{\perp 2}\left[1.2\sin^2\alpha\cos\alpha\right] - A_{\parallel}\left[0.083\cos\alpha\sin\alpha - 0.035\cos^2\alpha\sin\alpha\right]\right\}\hat{e}_Z\right]$$

Comparing the leading order terms of this result to the lift and drag relations in Figure 5 verifies that the clutter model recovers the independent lift and drag results of Hoerner[24] for a cylinder at angle of attack.

*Unidirectional Turbulent Flow in Porous Media*

Two limiting cases are under consideration for assessing the clutter model. The first is unidirectional flow in periodic porous media as illustrated in Figure 6.

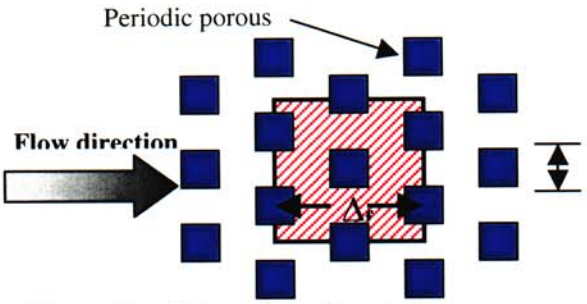


**Figure 6: Schematic of periodic porous media problem.**

Figure 7 (a) and (b) show predictions of normalized turbulent kinetic energy and its dissipation rate as a function of downstream locations using the macroscopic clutter model. The initial kinetic energy and dissipation rate are chosen to be 10 and 30 times the steady state values, respectively, in order to match the previous studies of the same problem from Nakayama *et al.*[4] and Pedras *et al* [1]. Predictions using the clutter model agree well with these previous studies in this limiting where the clutter model degenerates to just the porous media contribution.

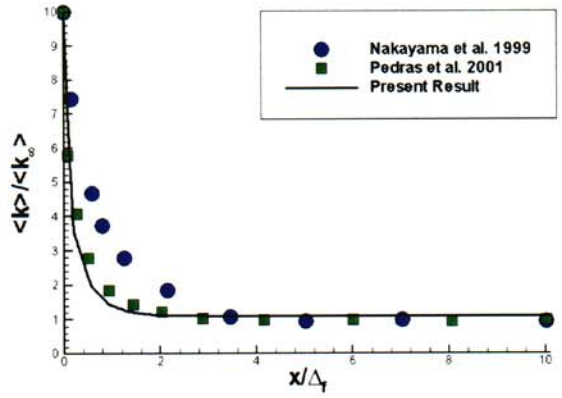


**(a)**

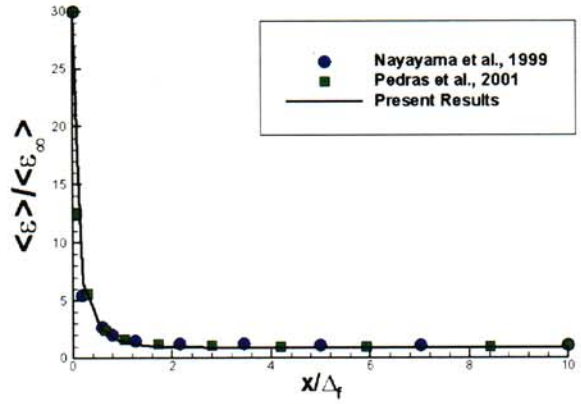


**(b)**

**Figure 7: Normalized turbulent kinetic energy and its dissipation rate verses $x/\Delta_f$ using clutter model in the limit of porous media.**

*Single Clutter Element in Turbulent Flow*

The second problem under consideration is a cylinder in well-characterized homogeneous turbulent flow. Experimental measurements are taken at the U.S. Naval Academy (USNA) using their low-speed (0 to 20 m/s) tunnel as shown in Fig. 8, for which high turbulence intensities could be generated at the inlet. Hot wire anemometry is used to measure instantaneous stream-wise velocity to obtain mean and RMS profiles before and after the cylinder.

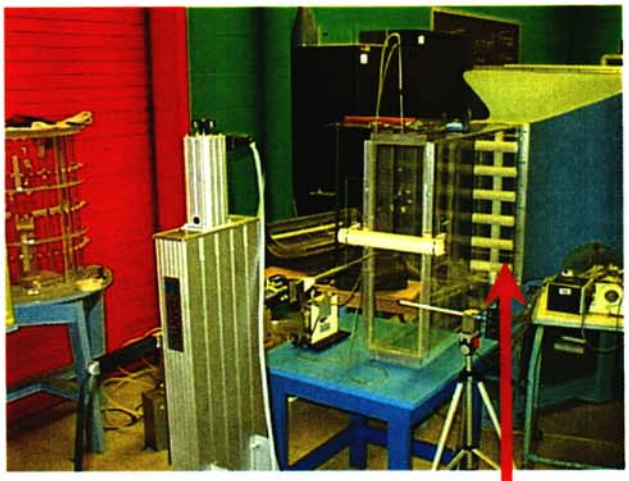

**(a)**

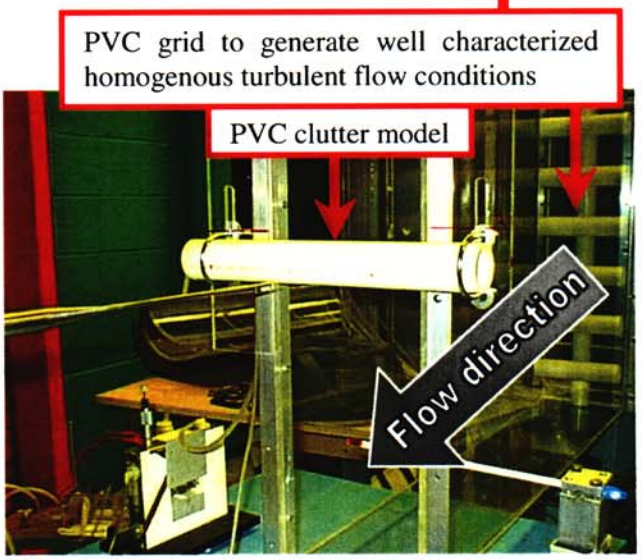


**(b)**

**Figure 8:: Pictures of (a) USNA wind tunnel facility and (b) blow up region of cylinder representing clutter object under highly turbulent flow conditions.**

One of the challenges in comparing the CFD predictions to hot-wire data is that hot-wire only measures the absolute value of velocity. This limitation becomes especially problematic in regions of the flow undergoing strong recirculation where the measured time-averaged velocity using hot-wire can be much larger than the actual velocity. Alternatively, one can compare the average of the velocity squared for which no ambiguity exists. Figure 9 show measurements (shown with symbols) of time-averaged velocity squared. This information is used in a momentum balance calculation to find the coefficient of drag ($C_D$) and is determined to be 0.97, which is ***24% lower*** than coefficient of drag of 1.28 determined with a turbulence intensity level of 2% without the turbulence generator in place. This result indicates that the effects of upstream turbulence on the drag characteristics of clutter are significant and should be included in future refinement of the clutter model.

Also in Figure 9 are several detailed 2D and 3D CFD predications using the CFD-ACE software package[32] (shown with lines). The purpose of conducting the detailed CFD calculations is to provide full flow field details to construct phase-averaged quantities that cannot be obtained experimentally. These details are needed for calibration of the unknown clutter model coefficient, $C_{k_B}$, in Eqs. (36) and (37) for the bluff body drag limit.

As shown in Figure 9, good qualitative agreement is obtained using 3D calculation while the 2D predictions tend to under-predict the extent of the velocity deficit profile for all of the turbulence models considered. These differences may be attributed to the limitations performing a 2D calculation when the flow has a strong 3D dimensional component of stream-wise vorticity generation. The 3D prediction using the RNG k-ε model shows good quantitative agreement to the experimental data just before and after the cylinder. However, the agreement tends to degrade further downstream. Similar results were obtained using a k-ω turbulence model. The current effort is to resolve these differences so that the detailed CFD calculations can be used to obtain phase-averaged stream-wise velocity and turbulent kinetic energy profiles as a function of downstream distance. This information will be compared to predictions to macroscopic model and will help determine the final modeling constants needed in the bluff body limit of the clutter model.

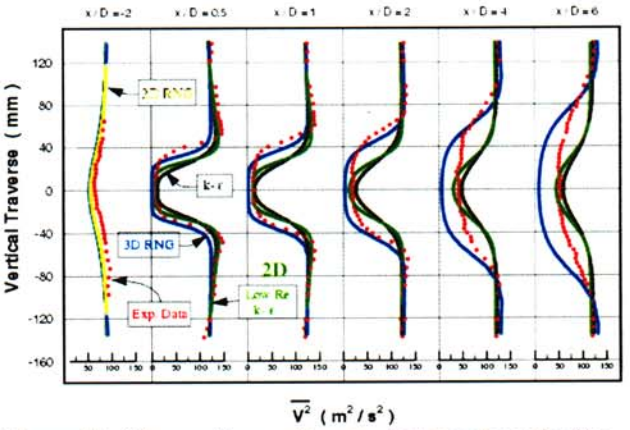


**Figure 9: Comparisons of mean streamwise velocity profiles at several down stream locations. Solid lines are CFD predictions and symbols are experimental measurements.**

## Conclusions

A preliminary clutter model has been formulated based on the use of two-phase averaging concepts. The implementation of phase averaging introduces constraints in the requirements of the clutter model. The most stringent of these constraints is that the model must be able to represent a wide range of clutter length scales ranging from a porous media limit to bluff body drag. This requirement is satisfied using a linear combination of constitutive models from the porous media literature and relations for bluff body drag. Based on this formulation, two simplified problems are considered for calibration of the model constants. The first is turbulent flow in a porous media for which a preliminary version of the clutter model is able to reproduce established trends taken from the literature. The second problem is cylinder in a highly turbulent cross flow for which there is little existing published data. Results of experimental measurements show a significant decrease in drag coefficient due to the highly turbulent inflow that will be important in future calibration of the model. Detailed numerical predictions of the same problem show good qualitative agreement to experimental measurements but quantitative differences exist. Future work is to perform this calibration so that the macroscopic model will be able to reproduce velocity deficit and turbulent kinetic energy production in the bluff body limit.

## Acknowledgments

The authors would like to thank Dr. Dave Keyser of Naval Air Systems Command for coordinating this activity. This research is part of the Department of Defense's Next Generation Fire Suppression Technology Program, funded by the DoD Strategic Environmental Research and Development Program.

## References


[1] Pedras, M. H. J. and de Lemos, M. J. S., "Macroscopic turbulence modeling for incompressible flow through undeformable porous media", *International Journal of Heat and Mass Transfer*, **44**, pp. 1081-1093, 2001.

[2] Pedras, M. H. J. and de Lemos, M. J. S., "Simulation of Turbulent Flow in Porous Media Using a Spatially Periodic Array and a Low Re Two-Equation Closure", *Numerical Heat* Transfer, **39**, pp. 35-39, 2001.

[3] Pedras, M. H. J. and de Lemos, M. J. S., "On the Definition of Turbulent Kinetic Energy for Flow in Porous Media", *Comm. Heat Mass Transfer*, **27**, pp.211-220, 2000.

[4] Nakayama, A. and Kuwahara, F., "A Macroscopic Turbulence Model for Flow in a Porous Medium", *Journal of Fluids Engineering*, **121**, pp. 427-433, 1999.

[5] Kuwahara, F., Kameyama, Y., Yamashita, S. and Nakayama, A., "Numerical Modeling of Turbulent Flow in Porous Media Using a Spatially Periodic Array", *Journal of Porous Media*, **1**, pp. 47-55, 1998.

[6] Antohe, B.V. and Lage, J.L., "A general two-equation macroscopic turbulence-model for incompressible flow in porous media", *Int. J. Heat Mass Transfer*, **40**, pp. 3013-3024, 1997.

[7] Kaviany, M., Principles of Heat Transfer in Porous Media, Springer-Verlag, New York, NY, 1991.

[8] Anderson, T. B. and Jackson, R., "A Fluid Mechanical Description of Fluidized Beds", *I&EC Fundamentals*, **6**, 1967.

[9] Gray, W. G. and Lee, P. C. Y., "On the Theorems for Local Volume Averaging of Multiphase Systems", *Int. J. Multiphase Flow*, **3**, pp. 333-340, 1977.

[10] Gough, P. S. and Zwarts, F. J., "Modeling Heterogeneous Two-Phase Reacting Flow", *AIAA Journal*, **17**, pp. 17-25,1979.

[11] Kuo, K. K., Principles of Combustion, A Wiley-Interscience Publication, John Wiley & Sons, New York, NY, 1986.

[12] Slattery, J.C., "Flow of viscoelastic fluids through porous media", *A.I.Ch.E. J.*, **13**, pp. 1066- , 1967.

[13] Slattery, J. C., momentum energy and mass transfer in continua, second edition, Robert E. Krieger Publishing Company, Inc., 1981.

[14] Kaplan, W., Advanced Calculus, Edition 3rd, Addison-Wesley Publishing Company, Reading, MA, pp. 257-259, 1984.

[15] Ghosal, S. and Moin, P., "Basic Equations for the Large Eddy Simulation of Turbulent Flow in Complex Geometry", *J. Comput. Phys.*, **118**, pp. 24-37, 1995.

[16] Ghosal, S., "Mathematical and Physical Constraints on Large-Eddy Simulation of Turbulence", *AIAA Journal*, **37**, 1999.

[17] Vailyev, O. V. , Lund, T.S. and Moin, P., "A General Class of Commutative Filters for LES in Complex Geometries," *Journal of Compuational Physics*, **146**, pp. 82-104, 1998.

[18] DesJardin, P.E and Gritzo, L.A., "On the Development of a Clutter Model for Turbulent Flows", SAND Report (in preparation), 2002.

[19] Tennekes, H. and Lumley, J.L., A First Course in Turbulence, MIT Press, Cambridge, MA, 1972.

[20] Pope, S.B., Turbulent Flows, Cambridge University Press, New York, NY, 2000.

[21] Brinkman, H. C., "A Calculation of the Viscous Force Exerted by a Flowing Fluid on a Dense Swarm of Particles", *Appl. Sci. Res.*, A1, pp. 27-34, 1947.

[22] Brinkman, H. C., "On the Permeability of Media Consisting of Closely Packed Porous Particles", *Appl. Sci. Res.*, A1, pp. 81-86, 1948.

[23] Blevins, R. D., Applied Fluid Dynamics Handbook, Van Nostrand Reinhold Company Inc., New York, NY, pp.333-334, 1984.

[24] Hoerner, S. F., Fluid-Dynamic Drag, published by author, New York, NY, 1957.

[25] Forchheimer, P. Z., Z. Ver. Deutsch Ing., vol. 45, pp. 1782, 1901.

[26] Ergun,, S., "Fluid flow through packed columns", *Chem. Eng., Prog.*, **48**, 89-94, 1952.

[27] Holen, J., Brostøm, M. and Magnussen, B.F., "Finite difference calculation of pool fires", In *Proceedings of 23rd Symp. (Int.) on Combustion*, 1677-1683, The Combustion Institute, Pittsburgh, PA, 1990.

[28] Jones, W.P. and Launder, B.E., "The prediction of laminarization with a two-equation model of turbulence", *Int. J. Heat Mass Transfer*, **15**, 301-314, 1972.

[29] Patankar, S.V., *Numerical Heat Transfer and Fluid Flow*, Hemisphere Publishing Co, New York, NY, 1980.

[30] Gritzo, L.A., Nicolette, V.F., Tieszen, S.R., Moya, J.L. and Holen, J., "Heat transfer to the fuel surface in large pool fires", In Chan, S.H., editor, *Transport Phenomena in Combustion*, pp. 701-712, Taylor & Francis, 1995.

[31] Gritzo, L.A. and Nicolette, V.F., "Coupling of large fire phenomenon with object geometry and object thermal response", *Journal of Fire Sciences*, **15**, 427-442, 1997.

[32] CFD-ACE™, CFD-ACE Structured Flow Solver Manual, Version 5, CFD Research Corporation, Huntsville, Alabama, October, 1998.